BMC Genomics

RESEARCH Open Access

Genome-wide identification and molecular characterization of the MAPK family members in sand pear (*Pyrus pyrifolia*)

Yue Xu[1], Huiying Wang[1] and Haiyan Shi[1*]

Abstract

Background 'Whangkeumbae', a highly regarded variety of sand pear, is celebrated in the market for its distinctive and superior flavor. However, the rapid production of ethylene after harvest significantly shortens its shelf life, becoming a major limiting factor for enhancing its commercial value. Mitogen-activated protein kinases (MAPKs) are a highly conserved family of transferases in eukaryotes. Although the importance of this family has been extensively studied in other plants, the precise composition and functional mechanisms of MAPK members in sand pear remain elusive. A genome-wide identification and molecular characterization of the *MAPK* gene family were conducted in *Pyrus pyrifolia*. This comprehensive analysis aimed to elucidate the genomic distribution, evolutionary relationships, and potential biological roles of *MAPK* genes in fruit senescence.

Results Four PpMAPKs were identified from our transcriptome data of sand pear, and 22 PpMAPK proteins were identified from the sand pear genome. Specifically, the transcriptomic PpMAPK3-L (GenBank accession number: PP992971), PpMAPK7-L (GenBank accession number: PP992972), PpMAPK10-L (GenBank accession number: PP992973), and PpMAPK16-L (GenBank accession number: PP992974) exhibited sequence homology values of 99.19%, 100%, 94.51%, and 95.75%, respectively, with their corresponding genomic counterparts (EVM0007944.1, EVM0004426.1, EVM0023771.1, EVM0027166.1). These findings indicate that the integrated analysis of transcriptomic and genomic data provides critical genetic insights into the *MAPK* genes in sand pear, culminating in the identification of a total of 25 *PpMAPK* genes in this species. Further phylogenetic analysis classified these genes into four subfamilies (A, B, C, and D), with subfamilies A and B each comprising six members, subfamily C with four members, and subfamily D with nine members. The potential functional differences among the gene members of each subfamily provide valuable clues for future research into MAPK signaling pathways. Further analysis by qRT-PCR revealed that the expression of four *PpMAPK* genes was positively correlated with fruit senescence in *Pyrus pyrifolia*. Additionally, interaction analysis revealed a significant interaction between PpMAPK3-L and PpbZIP2, which coordinatively regulate the senescence traits of fruits in sand pear through their joint influence during the senescence process.

Conclusion The results of this study suggest that *PpMAPK3-L*, *PpMAPK7-L*, *PpMAPK10-L*, and *PpMAPK16-L* are likely to play pivotal roles in the maturation and senescence of sand pear fruit. Specifically, the interaction between

*Correspondence:
Haiyan Shi
shyrainbow@aliyun.com

Full list of author information is available at the end of the article

PpMAPK3-L and PpbZIP2 could play a key role in the regulation of fruit senescence, indicating that the MAPK signaling pathway may modulate the fruit's physiological state through interactions with transcription factors. This finding offers significant insights for further investigation into the functions of *MAPK* genes in the maturation and senescence of sand pear fruit and provides a new direction for investigating biotechnological approaches for delaying senescence and prolonging shelf life.

Keywords *Pyrus pyrifolia*, MAPK, Molecular characterization, BZIP, Sand pear senescence

Background

Senescence is the final stage of fruit development [1]. This process causes a series of irreversible events, such as fruit softening, respiratory bursts, enhanced ethylene production, cell wall modifications, and color changes [2]. According to the difference in ethylene produced during ripening and senescence, fruits are divided into non-climacteric and climacteric. Those fruits with low ethylene production and no significant ethylene peak during ripening and senescence were non-climacteric fruits. In the process of ripening and senescence, ethylene increased rapidly in the climacteric fruit [3]. Sand pear (*Pyrus pyrifolia*) is a typical climacteric fruit, it has a short shelf life and rapid senescence after harvesting, which limits the development of its industry. Therefore, delaying the aging of sand pear fruit and extending the shelf life of sand pear is the key problem facing the sand pear industry.

Salicylic acid (SA), also known as 2-hydroxybenzoic acid, is a phenolic compound widely distributed in the plant kingdom. As a key signaling molecule and plant hormone, SA plays an essential role in various physiological processes in plants [4]. It is involved in fundamental physiological functions such as seed germination, photosynthesis, transpiration, stomatal regulation, thermogenesis, cell growth, and ion absorption. Moreover, SA plays a crucial role in the plant immune system, regulating both local and systemic defense mechanisms [5]. In recent years, SA has gained significant attention in the postharvest management of horticultural crops due to its remarkable effects in inhibiting senescence, delaying maturation, and enhancing resistance to various biotic and abiotic stresses [6]. Studies have shown that SA can significantly extend the shelf life of crops, reduce the incidence of diseases, and improve crop performance under adverse environmental conditions, highlighting its great potential in modern agriculture.

Mitogen-activated protein kinase (MAPK), as a specific serine/threonine protein kinase, is one of the largest transferases in eukaryotes [7]. Because this kinase is associated with a group of proteins that are phosphorylated by tyrosine residues under the action of mitogen, it is named mitogen-activated protein kinase. MAPK belongs to a multi-gene family. So far, MAPK family members have been identified in a variety of plants. Such as *Arabidopsis thaliana* [8], maize [9], corn [10], bananas [11], apples [12], tomatoes [13], and cucumbers [14].

The MAPK signaling pathway plays a crucial role in a variety of biological processes. MAPK can catalyze the phosphorylation of substrate proteins by transferring a phosphate group from ATP to the amino acid residues of the substrate proteins. MAPK cascade systems are widely present in eukaryotic organisms and play an important role in regulating cell growth and development and responding to external environmental stimuli [15]. It has been shown that MabZIP21 can interact with MaMPK6-3. The interaction between MaMPK6-3 and MabZIP21 enhanced the transcriptional activation of MabZIP21. Ser-436 and Thr-318 are the major phosphorylation sites of MabZIP21 by MaMPK6-3 [16]. In rice, MAPK5 can interact with OsWRKY72 to regulate the growth, development, and defense response of rice [17]. In tomato, the yeast two-hybridization (Y2H) experiment showed that SlASR4 protein interacts with SlMAPK3 protein, representing a class of proteins with conserved ABA/WDS domains and forming protein complexes capable of responding to various stresses [18]. In *Arabidopsis thaliana*, the phosphokinase MAPK6 phosphorylates ACS6 and increases its protein stability, thereby increasing ethylene production [19]. Currently, most research on MAPK is focused on stress resistance and morphogenesis. As an important protein kinase, MAPK must play an important regulatory role in the process of fruit senescence. However, there are very few research reports on this aspect. Understanding the mechanisms by which MAPK regulates fruit senescence, including the specific signal transduction pathways involved, remains a critical area of research in pomology. To reveal the relationship between MAPK signal and fruit shelf life, it is necessary to deeply analyze the unique role of MAPK signal in the sand pear fruit senescence process.

Transcription factors (TFs) play a crucial role in plant physiological processes, acting as key regulators in plant growth, development, and responses to environmental changes [20]. Among all transcription factor families, the basic leucine zipper (bZIP) family is one of the largest and most diverse. The name of the bZIP transcription factor is derived from its unique structural domain-the bZIP domain, which typically consists of 60 to 80 amino acids and contains two functional regions: a basic region and a leucine zipper region [21].

In bZIP proteins, the basic region consists of approximately 16 amino acid residues and contains a highly

conserved motif, N-x7-R/K-x9, which primarily functions in nuclear localization and DNA binding. In contrast, the leucine zipper region is composed of multiple heptad repeat motifs of amino acids, usually dominated by leucine (Leu), but may also include other large hydrophobic amino acids such as isoleucine (Ile), valine (Val), phenylalanine (Phe), or methionine (Met). Although the amino acid sequence in this region is more variable and not as highly conserved as the basic region, it plays a crucial role in protein dimerization. Specifically, the leucine zipper region is involved not only in the homodimerization of bZIP transcription factors but also in the formation of heterodimers with other transcription factors [22].

The *bZIP* gene family plays an indispensable role in various biological processes in plants. Extensive research has shown that bZIP transcription factors regulate plant growth, development, and responses to environmental stress. BZIP TFs control several aspects of plant development, particularly important growth events such as fruit ripening, and plant responses to environmental stress [23, 24]. For example, in peaches, the expression of *PpbZIP* genes is higher at the early stages of fruit maturation and gradually decreases as ripening progresses [25]. In lychees, several *bZIP* genes, including *LcbZIP17*, *LcbZIP4*, *LcbZIP5/7/21*, *LcbZIP2/19/28*, *LcbZIP9/32/33/44/53*, and *LcbZIP24/29/40/41*, are primarily expressed during the postharvest phase, participating in the regulation of fruit postharvest growth and maturation [26]. Additionally, the *bZIP11* gene in *Arabidopsis thaliana* influences root development by regulating the connection between low-energy signals and auxin-mediated primary root growth [27]. In maize, overexpression of the *ZmbZIP4* gene leads to increased lateral root numbers, elongation of primary roots, and a stronger root system [28]. In tomatoes, *SlbZIP33* (*SlAREB1*) not only participates in stress-induced responses but also regulates the expression of genes involved in critical metabolic pathways during fruit ripening, playing a key role in metabolic programming [29].

This study conducted an in-depth analysis of the transcriptomic and genomic data of the 'Whangkeumbae' (*Pyrus pyrifolia*) variety, 25 *PpMAPK* genes were identified in sand pear. These include four genes identified from the transcriptome and 22 genes discovered from the genome. To further explore the evolutionary relationships of these genes, a phylogenetic analysis was performed, revealing that these genes can be categorized into four major subfamilies (A, B, C, and D). Specifically, subfamilies A and B each contain six genes, subfamily C consists of four genes, and subfamily D, the largest, includes nine genes. These genes may have undergone varying degrees of functional differentiation during evolution, with potential functional differences among the subfamily members offering key insights into the mechanisms of the MAPK signaling pathway. Additionally, based on protein-protein interaction network analysis, the study identified that PpMAPK3-L interacts with the transcription factor PpbZIP2. This interaction may collaboratively regulate the fruit senescence process in sand pear during ripening, providing new perspectives on the molecular regulatory mechanisms of MAPK signaling during fruit maturation and senescence. These findings also present potential research directions for breeding sand pear varieties that delay fruit senescence.

Results

Identification and phylogenetic analysis of PpMAPK in sand pear

This study identified four PpMAPK from the transcriptome data [30] of sand pear, which were designated as PpMAPK3-L, PpMAPK7-L, PpMAPK10-L, and PpMAPK16-L. By comparing protein sequences in the genomic database [31], and removing duplicates and incomplete sequences, a total of 22 PpMAPK protein sequences were successfully identified in the sand pear genome. Among these genomic datasets, the sequence of PpMAPK3-L in the transcriptome exhibited a high similarity of 99.19% to that of EVM0007944 in the genome database. PpMAPK7-L was identical to EVM0004426, with a similarity of 100%. The sequence similarity between PpMAPK10-L and EVM0027166 was 94.51%, while PpMAPK16-L shared a similarity of 95.75% with EVM0023771. In summary, by integrating transcriptome and genomic data, a total of 25 PpMAPK were identified in the sand pear.

Based on this, the study further constructed a phylogenetic tree of the *PpMAPK* genes to reveal the evolutionary relationships between these genes. According to the classification criteria for the MAPK protein family in *Arabidopsis thaliana*. Based on the homology with *Arabidopsis thaliana* MAPK proteins and their amino acid sequence characteristics, the MAPK proteins were classified into four subgroups according to the classification standards for the MAPK protein family in *Arabidopsis thaliana*. (Fig. 1). The classification results indicate that the MAPK family members of *Arabidopsis thaliana* and sand pear are distributed across all subgroups. In subgroups A, B, and C, the MAPK proteins are of the TEY type, while those in subgroup D are of the TDY type. Specifically, subgroup A includes three *Arabidopsis* MAPK members and six sand pear MAPK members; subgroup B consists of four Arabidopsis MAPK members and six sand pear MAPK members; subgroup C comprises four Arabidopsis MAPK members and four sand pear MAPK members; subgroup D has the largest number of MAPK members, with nine MAPK members in both Arabidopsis and sand pear. The analysis of these data provides a

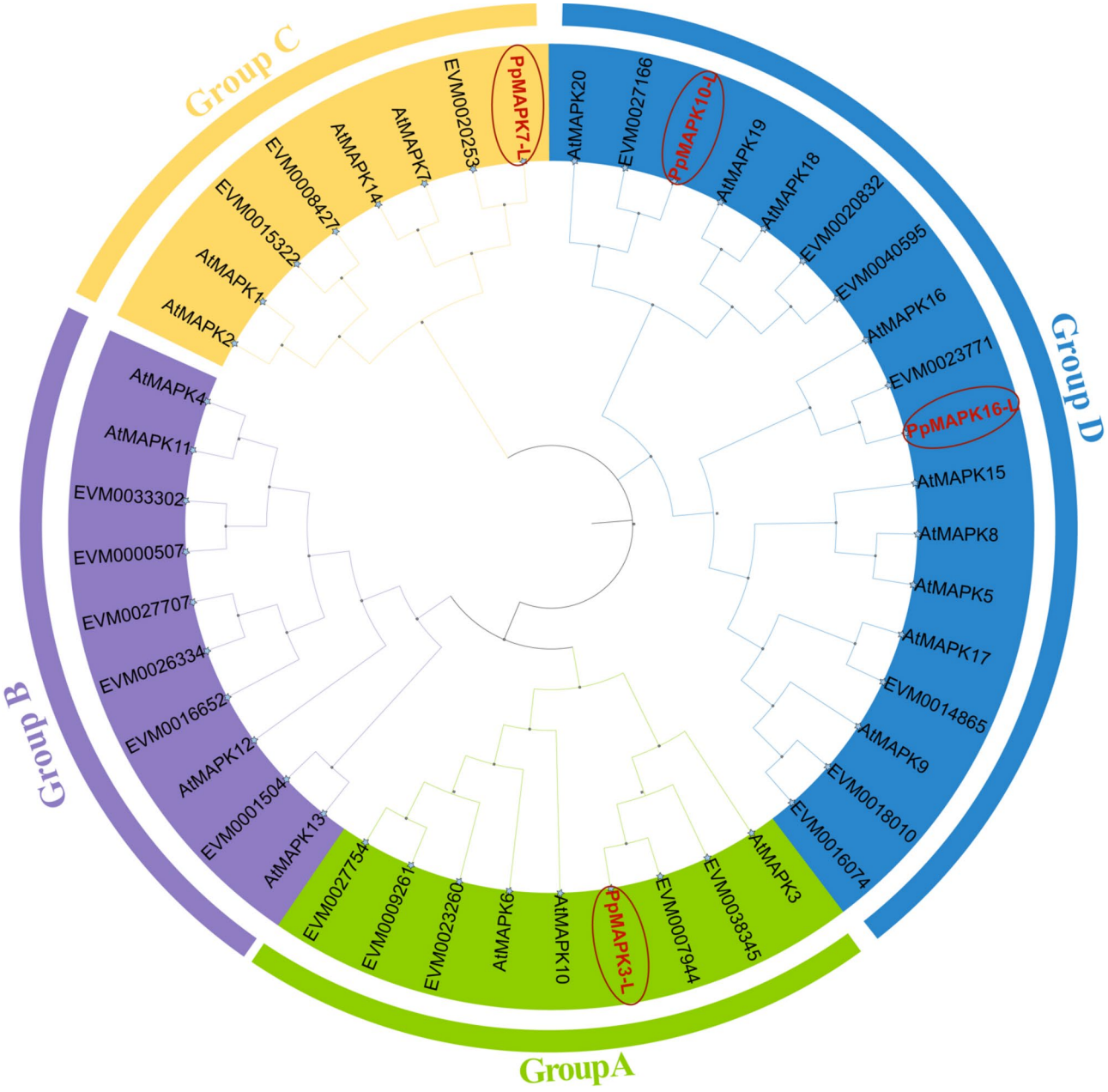

Fig. 1 Phylogenetic tree and classification of 25 members of the MAPK family of the sand pear genome. ClustalW method was applied to compare the amino acid sequence of 25 MAPK proteins, bootstrap analysis was performed on 1000 repeating sequences by NJ method, and the phylogenetic tree was constructed

clearer understanding of the classification and evolutionary characteristics of the sand pear MAPK family.

Phylogenetics, conserved motifs, domains, and gene structures of 22 PpMAPKs

Based on the obtained MAPK protein sequences, this study constructed a phylogenetic tree of the PpMAPKs and systematically analyzed their conserved motifs, conserved domains, and gene structures (Fig. 2). The analysis revealed that all PpMAPK protein sequences contain at least eight motifs. The shared motifs across each subfamily include motif 1, motif 2, motif 4, motif 5, motif 6, and motif 9. Notably, motif 6 is present in all protein sequences, indicating that this motif is highly conserved within the MAPK family. As a conserved motif of MAPKs, motif 6 is characterized by the sequence T(D/E)YVV(A)TRWYRAPEL, where the TxY part corresponds to the "T-loop" structure. This structural feature not only reflects the structural consistency of MAPK proteins but also suggests that PpMAPK possesses highly

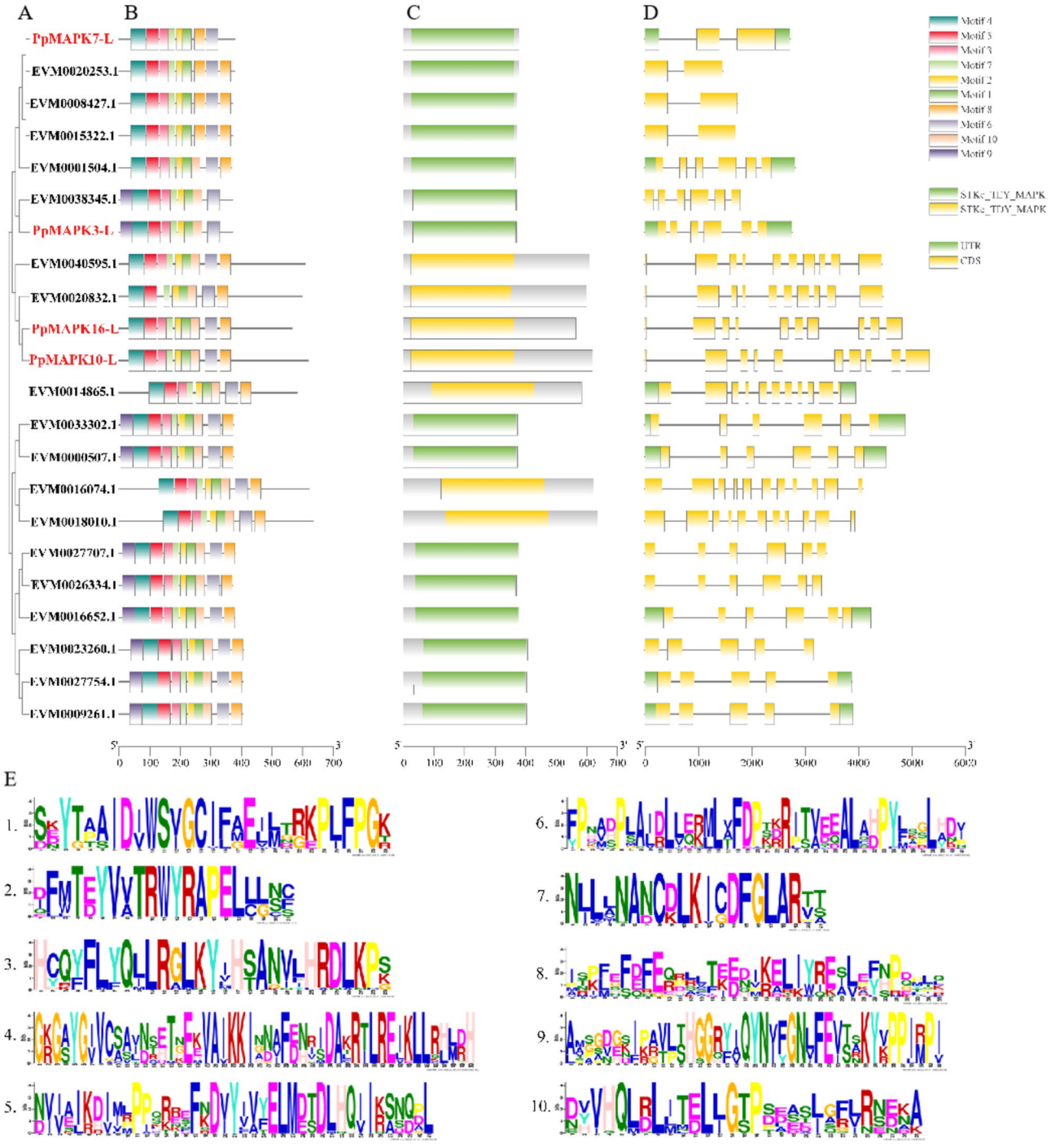

Fig. 2 Evolutionary relationship, conserved protein motif, domain and gene structure of PpMAPKs. **A** The phylogenetic tree was constructed based on protein sequences using the NJ method by MEGA7.0. **B-E** Motif compositions, domains and Exon/intron structures of the PpMAPKs

conserved functional characteristics. Motif 9 represents the CD domain, which plays an essential functional role in MAPK proteins (Fig. 2B). Subgroups A and B of the MAPK family possess a highly conserved CD domain, which has been maintained throughout evolution. This domain provides effective docking sites for upstream MAPKKs, protein phosphatases, and various substrate proteins, thereby serving as a critical molecular interface in signal transduction cascades. In contrast, members of subgroup C contain a modified version of the CD domain. Although structurally distinct, this domain retains functional significance and plays a pivotal role in regulating plant growth and development, including processes such as organogenesis, vegetative growth,

and hormonal signaling. Subgroup D members, on the other hand, lack a canonical CD domain and are primarily involved in mediating plant responses to abiotic stress. They are especially important in abscisic acid signaling and reactive oxygen species-induced stress responses.

The MAPK family functions as a central regulator in plant signal transduction pathways, facilitating the perception and transmission of various external stimuli. Through a hierarchical phosphorylation cascade, MAPKs activate downstream signaling components, thereby precisely modulating critical physiological processes such as cell growth, differentiation, senescence, and programmed cell death. To further explore the conserved domains of PpMAPK, this study employed the CD-search tool from the National Center for Biotechnology Information (NCBI) database for in-depth analysis. The results indicated that all 22 PpMAPK proteins in sand pear contain the MAPK domain, highlighting the high functional conservation of these proteins. PpMAPK proteins in subgroups A, B, and C share the same conserved domain (STKc_TEY_MAPK). TEY-type MAPKs phosphorylate their substrates in the nucleus, thereby facilitating signal transduction. PpMAPK proteins in subgroup D possess a distinct conserved domain (STKc_TDY_MAPK). (Fig. 2C). TDY is a unique feature of plant MAPKs. These MAPKs also play a role in regulating plant growth, development, and responses to various stress factors.

Further gene structure analysis showed a clear pattern in the number and distribution of exons and introns in *PpMAPK* genes. In particular, genes within the same evolutionary branch exhibited high similarity in exon and intron numbers and their distribution. All *PpMAPK* genes contain both introns and exons, with the *PpMAPKs* of the TDY type having relatively more exons, ranging from 9 to 11, with most genes containing 9 or 10 exons. The genes *EVM0014865*, *EVM0016074*, and *EVM00180* have the highest number of exons, reaching 11. In contrast, the *PpMAPKs* of the TEY type typically have fewer exons, usually ranging from 2 to 6, with the genes *EVM0020253*, *EVM0008427*, and *EVM0015322* having the fewest exons, with only 2. Additionally, 9 *PpMAPK* genes contain UTR regions, specifically *PpMAPK7-L*, *EVM0001504*, *PpMAPK3-L*, *EVM0014865*, *EVM0033302*, *EVM0000507*, *EVM0016652*, *EVM0027754*, and *EVM0009261*. These results suggest that the *PpMAPK* genes have undergone structural and functional diversification during their evolution (Fig. 2D).

Physicochemical properties and chromosomal localization of PpMAPKs

Through a systematic analysis of the physicochemical properties and related characteristics of 22 PpMAPK proteins, we observed significant differences in the number of amino acid residues in sand pear MAPK proteins (Table 1). Specifically, EVM0018010 has the largest number of amino acid residues, reaching 635, while EVM0001504 contains only 367, highlighting a significant difference between the two. Furthermore, the relative molecular mass of these proteins ranges from 42,064.88 Daltons (Da) to 71,683.59 Da, further indicating the structural diversity of PpMAPK proteins. In the isoelectric point (pI) analysis, the majority of PpMAPK proteins exhibited acidic characteristics, with 16 proteins having pI values lower than 7, indicating they are acidic proteins, while 6 proteins exhibited pI values above 7, indicating they are basic proteins. Notably, EVM0001504 had the lowest pI value of 5.06, making it the most acidic, while EVM0027166 and EVM0020832 both had pI values of 9.15, showing strong basic characteristics. Regarding protein instability, the instability index of PpMAPK proteins ranged from 31.11 to 48.19. Specifically, EVM0015322 exhibited the lowest instability index at 31.11, while EVM0000507 had the highest index at 48.19. The aliphatic amino acid index analysis revealed that PpMAPK16-L had the lowest index at 76.13, while EVM0020253 had the highest at 97.49. Hydrophilicity analysis showed that the GRAVY values of all PpMAPK family members were negative, further confirming that they are hydrophilic proteins. Subcellular localization prediction results showed that these proteins were all located in the nucleus, which was consistent with the subcellular localization of IbMPK3/6 in sweet potato [32], suggesting that they may be involved in signal transduction and regulation in the nucleus.

To further explore the distribution of *PpMAPK* gene family members in the genome, we conducted chromosome mapping and visualization analysis using TBtools software (Fig. 3). The analysis revealed that the *PpMAPK* genes are randomly distributed across 11 chromosomes of the sand pear genome, located on chromosomes 1, 2, 3, 6, 7, 8, 9, 11, 13, 14, and 15. However, the gene *EVM0026334* could not be successfully mapped to any chromosome. The distribution of *PpMAPK* genes on each chromosome showed significant variation, with the highest number of genes found on chromosomes 2, 11, and 15, each containing three genes. On other chromosomes, the number of *PpMAPK* genes was relatively low, particularly on chromosomes 1, 7, 8, and 9, which each contained only one *PpMAPK* gene: *EVM0000507*, *EVM0033302*, *EVM0008427*, and *PpMAPK10-L*, respectively. These results indicate an uneven distribution of *PpMAPK* genes in the sand pear genome, with the majority of genes located on specific chromosomes. This provides important genomic insights for further studying the functions and evolution of *PpMAPK* genes.

Table 1 The characterizations of PpMAPKs in sand pear

Gene name	Gene ID	Accession no.	Amino acids No.	Mw(Da)	pI	Instability index	Aliphatic index	GRAVY	Subcellular localization
	EVM0008427	GWHPBAOS037580	372	42582.21	5.96	34.86	95.70	-0.227	Nucleus
	EVM0015322	GWHPBAOS017334	372	42605.31	6.38	31.11	96.21	-0.234	Nucleus
MAPK7-L (GenBank accession number: PP992972)	EVM0004426(100%)	GWHPBAOS023153	379	43546.59	8.30	36.76	95.46	-0.203	Nucleus
	EVM0020253	GWHPBAOS015187	378	43357.27	7.26	37.45	97.49	-0.176	Nucleus
	EVM0033302	GWHPBAOS034299	373	42945.09	6.03	46.15	89.65	-0.369	Nucleus
	EVM0000507	GWHPBAOS001398	373	42962.96	6.02	48.19	89.12	-0.365	Nucleus
	EVM0016652	GWHPBAOS032599	378	43139.22	6.17	44.93	88.52	-0.335	Nucleus
	EVM0027707	GWHPBAOS012688	379	43147.21	5.97	43.26	89.31	-0.299	Nucleus
	EVM0026334	GWHPBAOS040261	370	42064.88	5.87	41.72	88.86	-0.305	Nucleus
	EVM0001504	GWHPBAOS005430	367	42183.22	5.06	39.39	95.91	-0.257	Nucleus
	EVM0038345	GWHPBAOS025676	370	42557.05	5.79	41.29	94.38	-0.259	Nucleus
MAPK3-L (GenBank accession number: PP992971)	EVM0007944 (99.19%)	GWHPBAOS005442	370	42626.93	5.62	39.72	92.54	-0.32	Nucleus
	EVM0027754	GWHPBAOS024101	403	46322.92	5.90	41.59	85.21	-0.361	Nucleus
	EVM0009261	GWHPBAOS024083	403	46293.93	5.83	41.60	85.46	-0.346	Nucleus
	EVM0023260	GWHPBAOS016125	406	46384.87	5.66	42.74	86.75	-0.313	Nucleus
	EVM0016074	GWHPBAOS011680	621	70605.48	6.54	37.90	77.28	-0.648	Nucleus
	EVM0018010	GWHPBAOS031618	635	71683.59	6.36	38.07	76.65	-0.603	Nucleus
	EVM0014865	GWHPBAOS011287	583	66525.65	6.59	45.10	81.63	-0.494	Nucleus
MAPK16-L (GenBank accession number: PP992974)	EVM0023771 (95.75%)	GWHPBAOS009972	564	63919.95	8.73	36.68	76.13	-0.502	Nucleus
MAPK10-L (GenBank accession number: PP992973)	EVM0027166 (94.51%)	GWHPBAOS038791	618	70715.07	9.15	34.31	80.19	-0.486	Nucleus
	EVM0040595	GWHPBAOS024513	608	68982.2	9.04	38.51	80.53	-0.458	Nucleus
	EVM0020832	GWHPBAOS006687	598	67812.97	9.15	38.37	79.93	-0.438	Nucleus

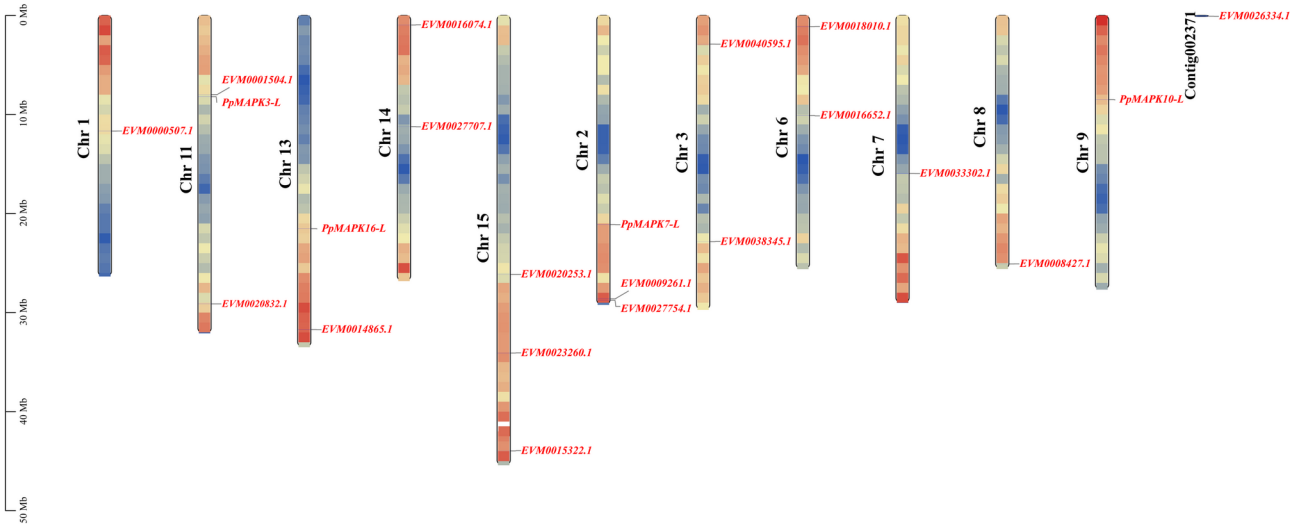

Fig. 3 Chromosome mapping of *PpMAPKs* in sand pear

Cis-element analysis of *PpMAPK* gene promoters

To investigate the functional roles of the *PpMAPK* gene family in greater depth, we extracted the 2 kb upstream sequences of 22 *PpMAPK* genes in sand pear and conducted a systematic analysis of their hormone-responsive cis-regulatory elements (Fig. 4). Notably, no hormone response elements were identified in the upstream sequence of the *EVM0020832* gene. In contrast,

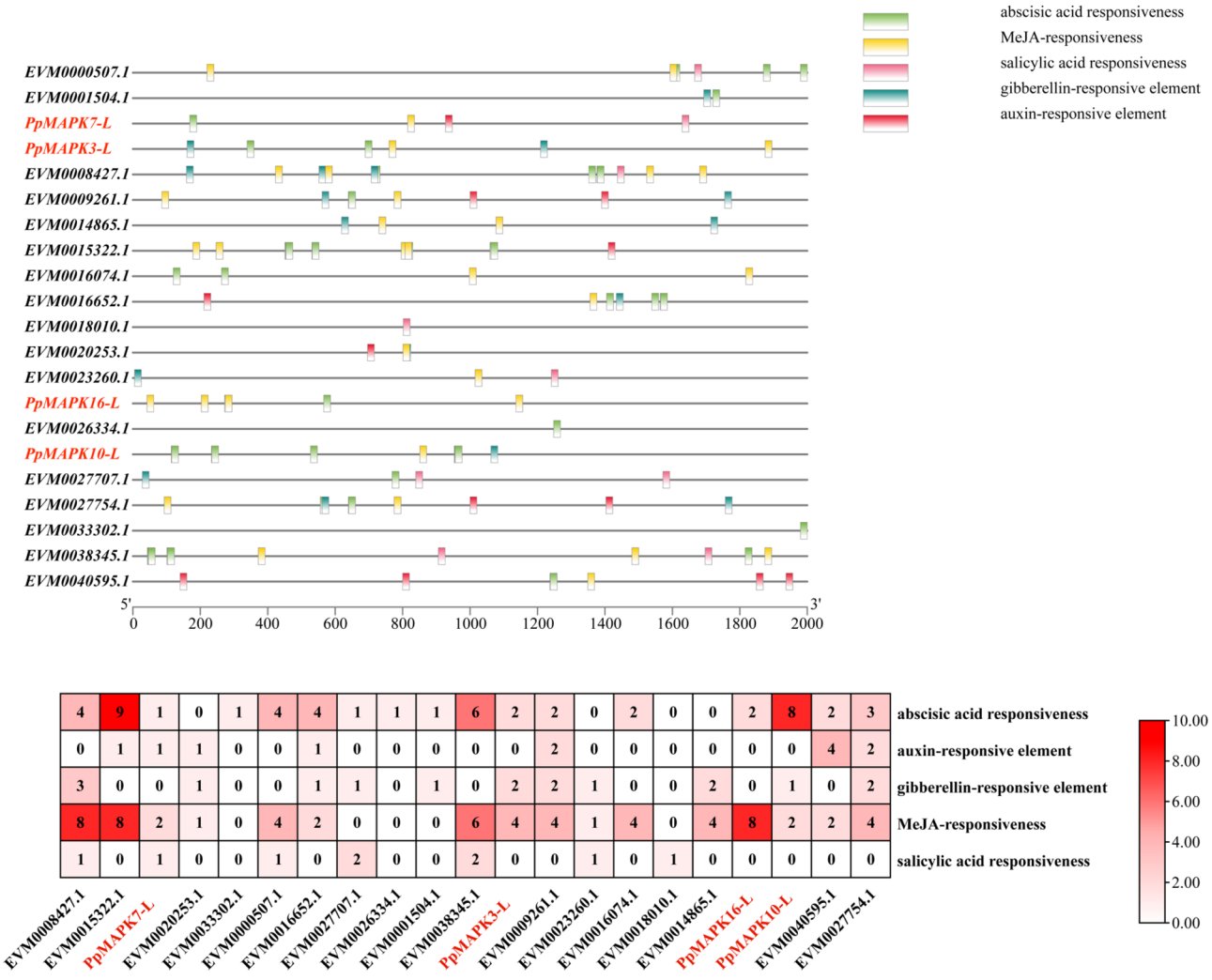

Fig. 4 Identification of cis-acting elements in the promoter region of *PpMAPK* genes. **A** Types of hormone-responsive cis-acting elements contained in *PpMAPKs*. **B** The numbers of cis-acting components that *PpMAPKs* contain

the upstream sequences of the remaining 21 *PpMAPK* genes contain five distinct types of hormone-responsive cis-regulatory elements, namely abscisic acid, auxin, gibberellin, jasmonic acid, and SA response elements. Among these five hormone response elements, the abscisic acid response element was the most common. Except for *EVM0020253*, *EVM0023260*, *EVM0018010*, and *EVM0014865*, nearly all *PpMAPK* genes contain this element. The auxin response element, on the other hand, was relatively rare and was found in only seven genes, including *EVM0015322*, *PpMAPK7-L*, *EVM0020253*, *EVM0016652*, *EVM0009261*, *EVM0040595*, and *EVM0027754*. The gibberellin response element, however, was more widely distributed, being present in the promoter sequences of 11 genes: *EVM0008427*, *EVM0020253*, *EVM0016652*, *EVM0027707*, *EVM0001504*, *PpMAPK3-L*, *EVM000926*, *EVM0023260*, *EVM0014865*, *PpMAPK10-L*, and *EVM0027754*.

The Methyl Jasmonate response element also showed a relatively broad distribution, with only a few genes lacking this cis-regulatory element: *EVM0033302*, *EVM0027707*, *EVM0026334*, *EVM0001504*, and *EVM0018010*. The SA response element, however, was more limited in distribution, being present in only seven genes: *EVM0008427*, *PpMAPK7-L*, *EVM0000507*, *EVM0027707*, *EVM0038345*, *EVM0023260*, and *EVM0018010*. In conclusion, the presence of various hormone-responsive cis-regulatory elements in the *PpMAPK* gene family of sand pear suggests that these genes may play important roles in plant hormone signaling pathways. The different hormone response elements likely reflect the functional differences of these genes in various physiological processes.

Expression patterns of *PpMAPKs* in sand pear (*Pyrus pyrifolia*)

Specific quantitative primers for *PpMAPK3-L*, *PpMAPK7-L*, *PpMAPK10-L*, and *PpMAPK16-L* genes were designed based on transcriptome data, with their primers provided in Additional file 1 (Table S1). Using these primers, detailed expression pattern analyses of the four *PpMAPK* genes were conducted across different tissue types (Fig. 5). The results revealed significant tissue-specific expression of the *PpMAPK* genes. Specifically, *PpMAPK3-L* exhibited the highest expression in petals and the lowest in leaves (Fig. 5A). *PpMAPK7-L* showed the lowest expression in leaves but peaked in shoot tips (Fig. 5B). *PpMAPK10-L* was predominantly expressed in anthers, with minimal expression in leaves (Fig. 5C). Similarly, *PpMAPK16-L* exhibited the weakest expression in leaves but showed the strongest expression in shoots (Fig. 5D). Furthermore, all four *PpMAPK* genes were expressed to varying degrees in fruit tissues, suggesting their potential involvement in fruit development.

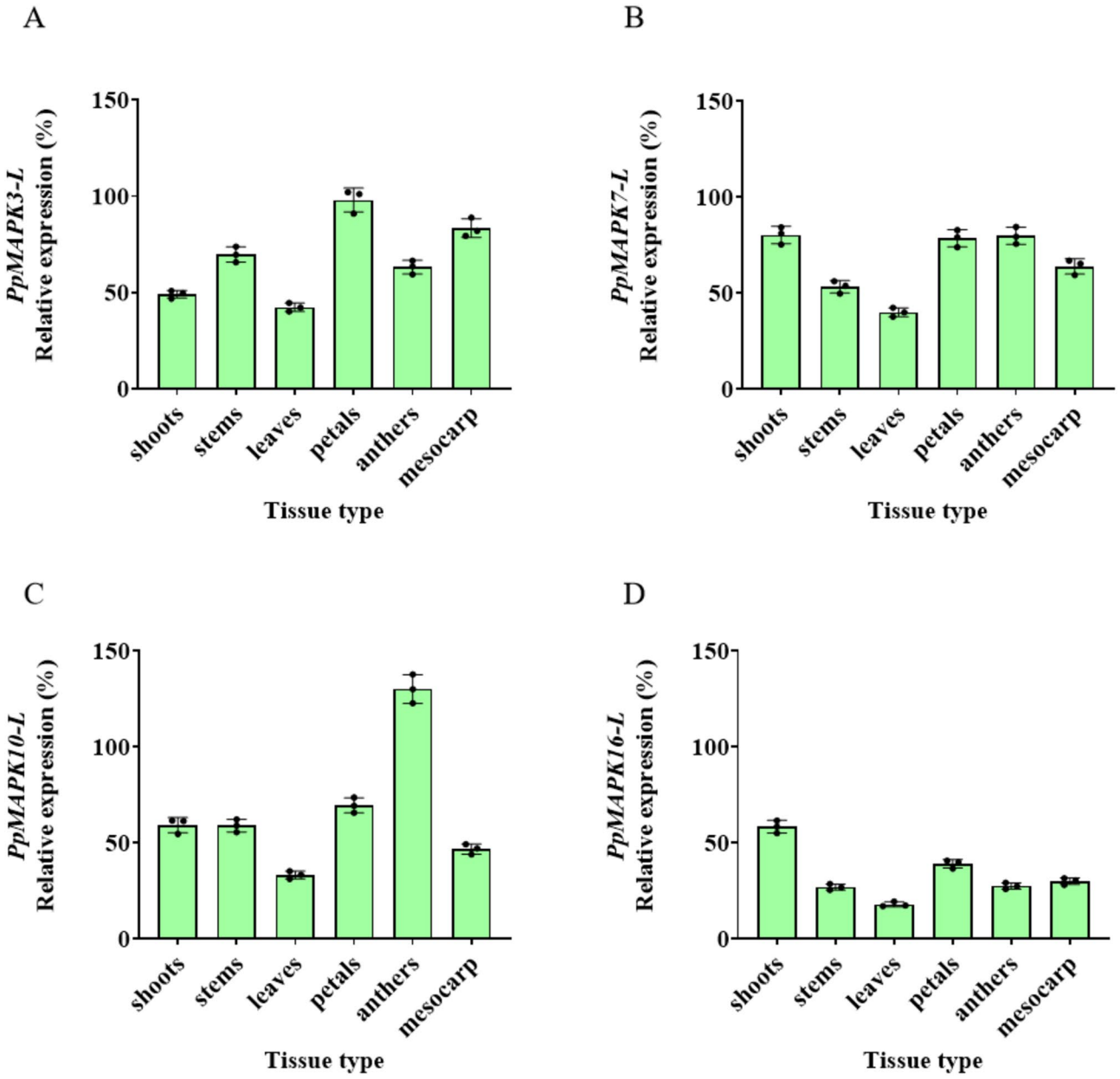

Fig. 5 Expression patterns of *PpMAPK3-L*, *PpMAPK7-L*, *PpMAPK10-L* and *PpMAPK16-L* in 'Whangkeumbae' tissue. The X-axis in the figure represents different tissue types collected from 'Whangkeumbae', including shoots, stems, leaves, petals, anthers, and mesocarp. The Y-axis indicates the relative expression levels of the *PpMAPKs* genes. The results are presented as percentages relative to *PpUBI* expression levels. The data shown are derived from three biological replicates, with the results expressed as means ± SD as error bars

To further explore the roles of *PpMAPK* genes in fruit development, their expression patterns were dynamically tracked across different stages of fruit development (Fig. 6). The results indicated that these genes were expressed post-harvest, each displaying distinct expression peaks. Specifically, *PpMAPK3-L* and *PpMAPK10-L* reached their highest expression levels 25 days after harvest (DAH), while *PpMAPK7-L* peaked at 30 DAH. In contrast, *PpMAPK16-L* exhibited its highest expression as early as 5 DAH.

Regulatory analysis of *PpMAPK* genes by SA and ETH

To explore the potential roles of *PpMAPK* genes in the process of fruit senescence, pears were treated post-harvest with different concentrations of SA: 0.002, 0.02, 0.2, and 2 mM (Fig. 7A, B, C, D). The expression of the four *PpMAPK* genes was then monitored. The experimental results showed that at a concentration of 0.002 mM SA, no significant differences in the expression levels of the four *PpMAPK* genes were observed compared to the control group. Under the 0.02 mM SA treatment, the expression level of *PpMAPK10-L* significantly increased, suggesting that it may play an important regulatory role under this condition. In contrast, the expression changes of other *PpMAPK* genes were relatively small. When the SA concentration was increased to 0.2 mM, only *PpMAPK3-L* exhibited significantly higher expression compared to the control group, suggesting that this concentration of SA may stimulate the expression of *PpMAPK3-L*, while the expression levels of the other three genes (*PpMAPK7-L*, *PpMAPK10-L*, and *PpMAPK16-L*) showed no significant differences from the control, indicating that these genes might be less sensitive or less responsive to this concentration of SA. At 2 mM SA, the expression of *PpMAPK3-L* was significantly lower than that of the control group, suggesting that this high concentration of SA may inhibit the expression of *PpMAPK3-L*. In contrast, *PpMAPK7-L* exhibited significantly higher expression, indicating that this concentration of SA may upregulate *PpMAPK7-L* expression

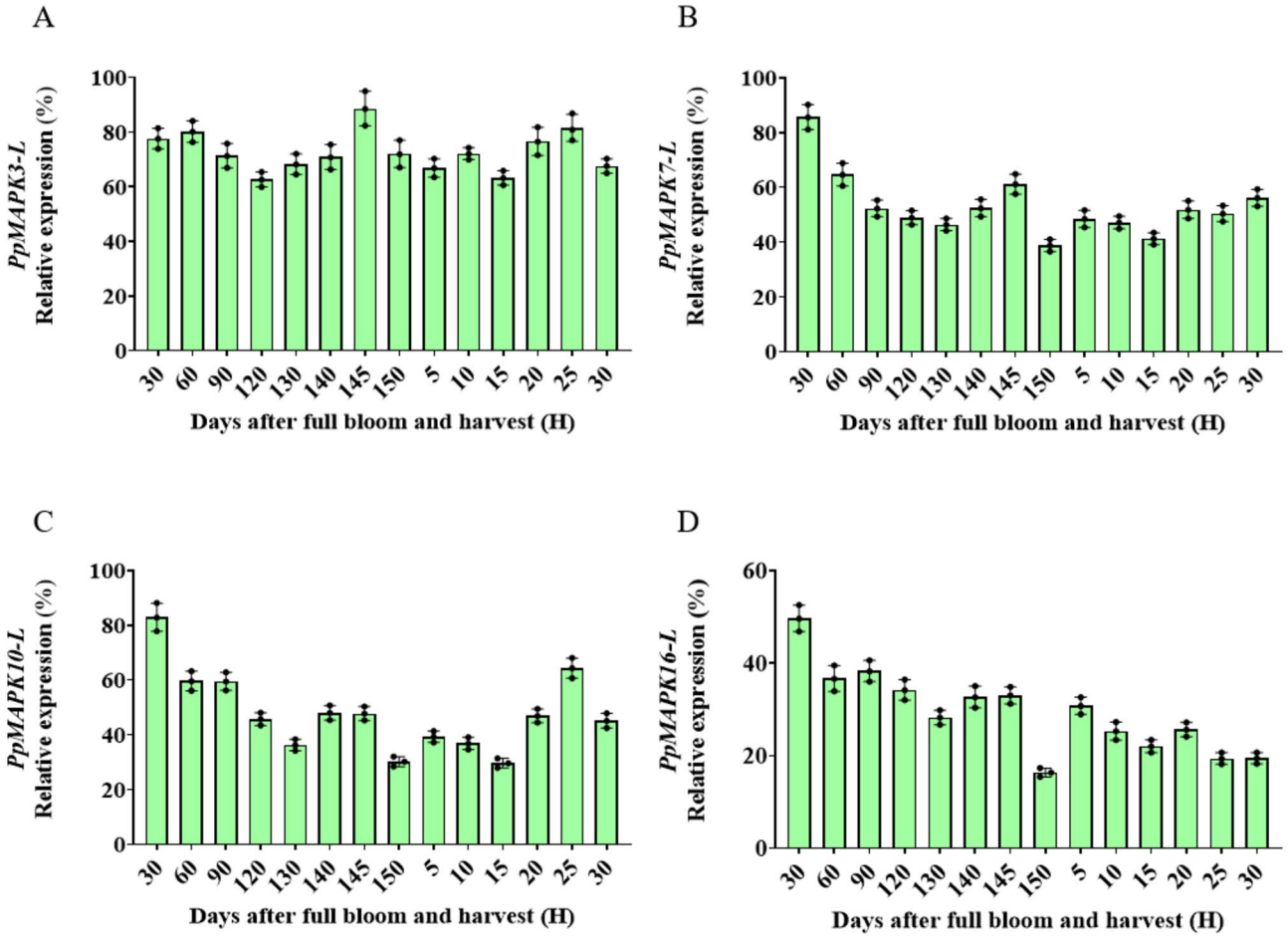

Fig. 6 Expression levels of *PpMAPK3-L*, *PpMAPK7-L*, *PpMAPK10-L* and *PpMAPK16-L* in 'Whangkeumbae'during fruit development. The X-axis in the figure represents samples of the 'whangkeumbae' fruit at different stages of development, including 30, 60, 90, 120, 130, 140, 145,150 DAFB and 5, 10, 15, 20, 25, 30 DAH. The y axis shows the relative expression levels of *PpMAPK* genes. The results are presented as percentages relative to *PpUBI* expression levels. The data shown are derived from three biological replicates, with the results expressed as means ± SD as error bars

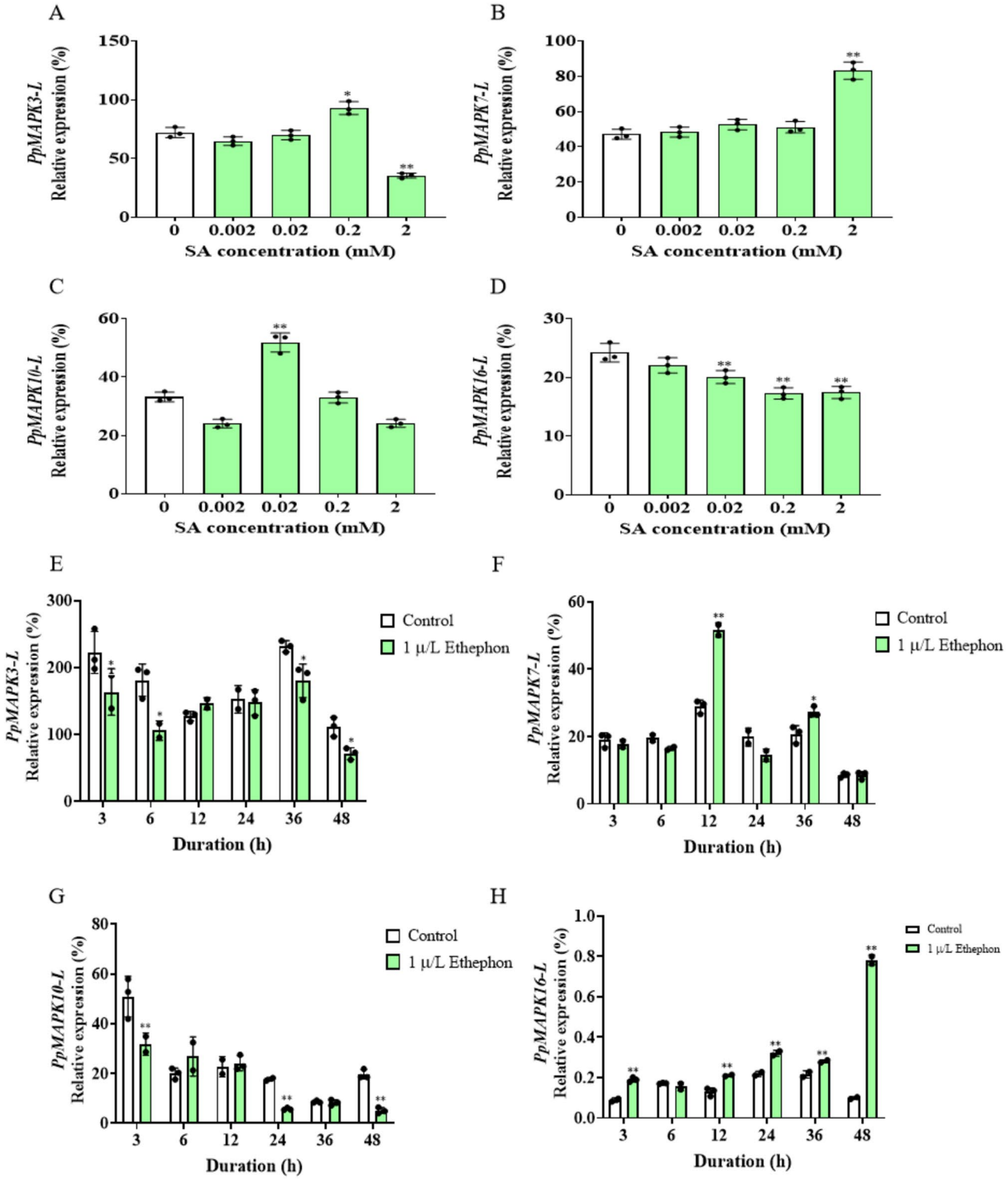

Fig. 7 SA and ETH regulate the expression of *PpMAPK3-L*, *PpMAPK7-L*, *PpMAPK10-L* and *PpMAPK16-L*. The X-axis in the figure represents samples treated with 0, 0.002, 0.02, 0.2, and 2 mM SA for 12 h, and with 1 μL/L ETH for 3, 6, 12, 24, 36, and 48 h in the fruit flesh of 'Whangkeumbae'. The Y-axis indicates the relative expression levels of the *PpMAPK* genes. Data are expressed as percentages relative to *PpUBI* expression levels. The results shown are derived from three independent biological replicates, with data presented as means ± SD and error bars representing the variability of the expression. Statistical significance is indicated by "*" ($P < 0.05$), and highly significant differences are denoted by "**" ($P < 0.01$)

through some mechanism. However, the expression of *PpMAPK10-L* and *PpMAPK16-L* did not differ significantly from the control group, suggesting that these two genes might be less responsive or unaffected by the 2 mM SA treatment.

To further elucidate the role of *PpMAPK* genes in fruit senescence and based on previous experimental designs, the flesh of post-harvest 'Whangkeumbae' pear was treated with 1 μ/L ethephon (ETH), and the expression of *PpMAPK* genes was analyzed at 3, 6, 12, 24, 36, and 48 h after treatment (Fig. 7E, F, G, H). The results showed that the expression of *PpMAPK3-L* was significantly lower at 3, 6, 36, and 48 h post-treatment compared to the control group, suggesting that ETH may inhibit the expression of this gene through some mechanism. The expression of *PpMAPK7-L* was significantly higher at 12 h post-treatment and also showed a significant increase at 36 h, indicating that ETH may activate the expression of this gene after prolonged treatment. The expression of *PpMAPK10-L* was significantly higher at 3, 24, and 48 h post-treatment, suggesting that ETH may participate in the fruit senescence process by up-regulating the expression of this gene at these time points. Finally, the expression of *PpMAPK16-L* was significantly increased at all time points (3, 12, 24, 36, and 48 h) after ETH treatment, indicating that ETH treatment may enhance the role of *PpMAPK16-L* in fruit senescence.

Interaction between PpMAPK3-L and PpbZIP2

Based on the aforementioned experimental results, the four PpMAPK genes each play distinct roles in fruit senescence. To further investigate the potential interaction mechanisms of these MAPKs during fruit senescence, we employed the online tool STRING to predict their potential interacting proteins. The prediction results suggested that PpMAPK3-L may interact with PpbZIP2 (Gene ID: EVM0004317.1), while PpMAPK7-L, PpMAPK10-L, and PpMAPK16-L may interact with PpbZIP3 (Additional file 2: Fig. S1).

To further confirm these predictions, we established a Y2H system to analyze the interactions between PpMAPK and PpbZIP. PpMAPK3-L, PpMAPK7-L, PpMAPK10-L, and PpMAPK16-L were individually cloned into the pGBKT7 (BD) vector to generate the recombinant vectors PpMAPK-BD. Concurrently, PpbZIP2 and PpbZIP3 were cloned into the pGADT7 (AD) vector to yield the recombinant vectors PpbZIP-AD. Initially, self-activation assays were conducted to verify that the constructed vectors did not possess the ability to spontaneously activate transcription. The experimental results demonstrated that after co-transforming the four PpMAPK-BD and PpbZIP-AD vectors, cells were able to grow normally on synthetic dropout medium/-tryptophan/-leucine (SD/-Leu/-Trp) medium, confirming the successful introduction of these genes into AH109 competent cells. Further tests revealed no growth on SD/-Trp/-Leu/-histones/-adenine/X-alpha gal (SD/-Trp/-Leu/-His/-Ade/X-α-gal) medium, confirming the absence of self-activation in the PpMAPK genes (Additional file 3: Fig. S2). Next, after co-transforming the four PpMAPK-BD vectors with the two PpbZIP-AD vectors into AH109 cells, the results revealed normal growth on SD/-Leu/-Trp medium, confirming the successful introduction of PpMAPK and PpbZIP into the competent cells. Among these experiments, only PpMAPK3-L-BD and PpbZIP2-AD exhibited significant growth on SD/-Leu/-Trp/-Ade/-His medium, further confirming the existence of an interaction between PpMAPK3-L and PpbZIP2. This study offers compelling evidence for understanding the molecular mechanisms of PpMAPK and PpbZIP proteins in fruit senescence and provides new insights for future functional research and regulation of fruit senescence (Fig. 8).

Expression Pattern of *PpbZIP2*

To further investigate the interaction mechanism between *PpMAPK3-L* and *PpbZIP2*, this study comprehensively analyzed the expression pattern of *PpbZIP2*. The results revealed that *PpbZIP2* is expressed in various tissues of sand pear, with the highest expression observed in the leaves and the lowest in the petals. This suggests that *PpbZIP2* may play distinct physiological roles in different tissues (Fig. 9A). To explore the role of *PpbZIP2* during fruit development, the expression dynamics of *PpbZIP2* throughout fruit development were monitored. The analysis showed that the expression of *PpbZIP2* fluctuated during fruit development, peaking at 30 DAH and reaching its lowest level of 60 days after full bloom (DAFB) (Fig. 9B). Notably, the expression of *PpbZIP2* is induced by SA (Fig. 9C), while ETH significantly inhibits its expression (Fig. 9D). This finding provides crucial insights into the role of *PpbZIP2* in fruit senescence and reveals potential molecular mechanisms by which SA and ETH regulate *PpbZIP2* expression.

Discussion

Mitogen-activated protein kinases (MAPKs) constitute a highly conserved family of serine/threonine protein kinases in eukaryotes, playing critical roles in plant growth, development, and signal transduction. *MAPK* gene families have been identified in various plant species, including rice [33], maize [9], chickpea [34], kiwifruit [35], barley [36], *Gossypium raimondii* [37], bread wheat [38], *Fragaria vesca* [39], *Fagopyrum tataricum* [40], *Brachypodium distachyon* [41], tomato [13], tobacco [42], poplar [43], apple [12], soybean [44] with varying numbers of family members (Additional file 4: Table S2). This indicates that, although the MAPK signaling

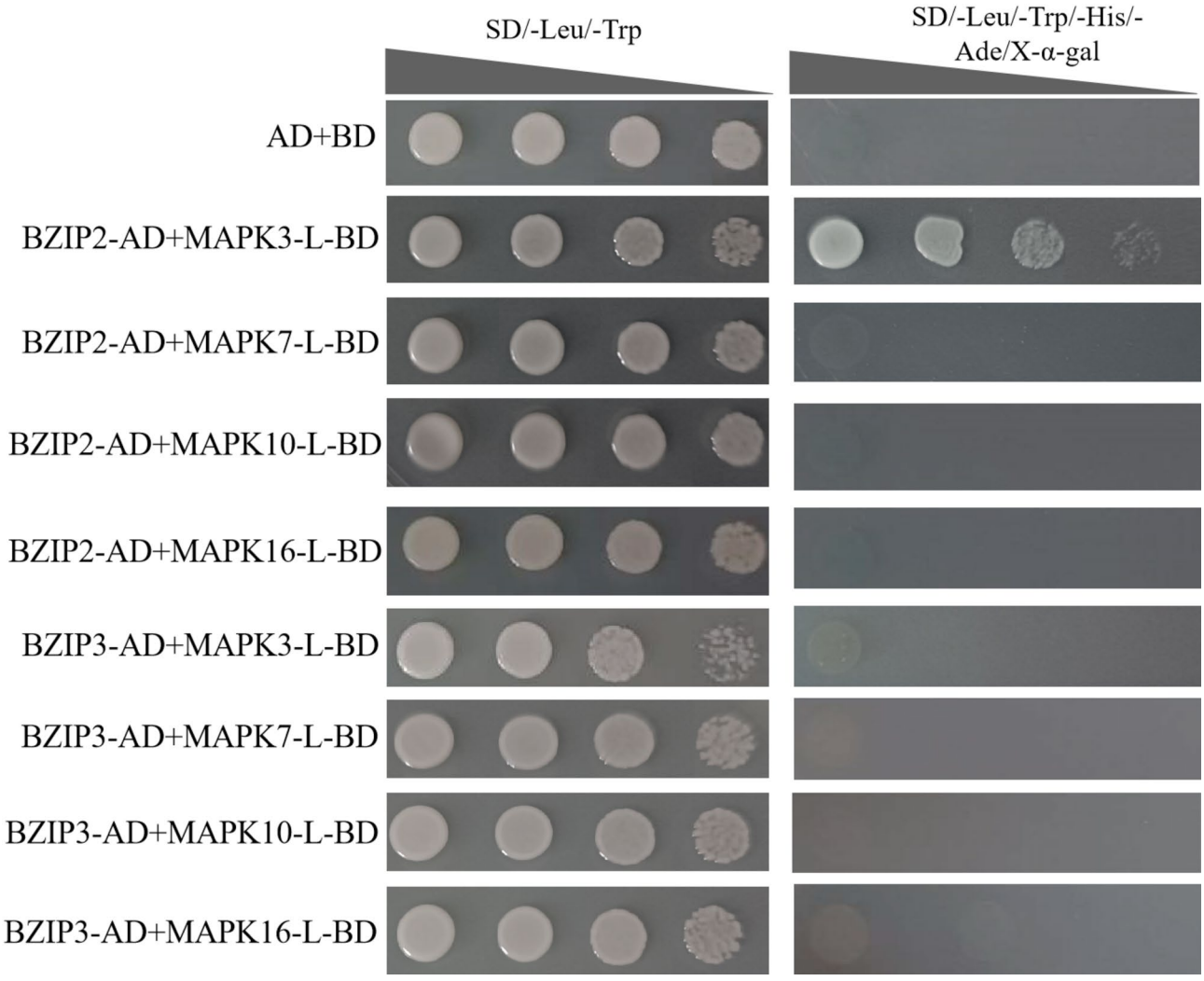

Fig. 8 Protein-protein interactions between PpMAPKs and PpbZIPs. In the yeast two-hybrid experiment, PpbZIPs-AD + BD, PpMAPKs-BD + AD, PpbZIPs-AD + PpMAPKs-BD were cultured on SD/-Leu/-Trp selective medium, respectively. The positive clones were inoculated in SD/-Trp/-Leu/-Ade/-His medium, and X-α-gal was added for interaction detection

pathway is highly conserved in eukaryotes, the evolution and function of its family members exhibit considerable species-specific variation. In this study, four *PpMAPK* genes were initially identified from the transcriptome of sand pear (*Pyrus pyrifolia*) and named *PpMAPK3-L*, *PpMAPK7-L*, *PpMAPK10-L*, and *PpMAPK16-L*. Subsequently, using 20 *Arabidopsis thaliana* MAPK protein sequences (AtMAPK1-AtMAPK20) as query sequences [8], an additional 22 MAPK family members were identified in the sand pear genome database through BLAST comparison and domain validation. The results revealed that PpMAPK7-L shows a 100% similarity with the EVM0004426 sequence in the genome. Based on the combined transcriptomic and genomic data analysis, a total of 25 *PpMAPK* genes were identified in sand pear, providing a solid foundation for a comprehensive study of the PpMAPK family. Comparative analysis revealed a remarkable diversity of *MAPK* genes across plant species.

MAPK gene families have been widely identified in various plant species, exhibiting complex expression patterns. The expression levels of these genes vary significantly between species, developmental stages, and tissue types. This study systematically investigated the expression patterns of the *PpMAPK* gene family across different tissues, revealing distinct tissue-specific expression profiles. Specifically, *PpMAPK3-L* is highly expressed in the petals, potentially involved in the regulation of floral organ development; *PpMAPK7-L* shows relatively prominent expression in the aerial parts of the plant, suggesting its role in the physiological processes in aerial tissues. Moreover, *PpMAPK10-L* is predominantly expressed in the anthers, possibly involved in pollen formation or anther development. *PpMAPK16-L* exhibits the highest

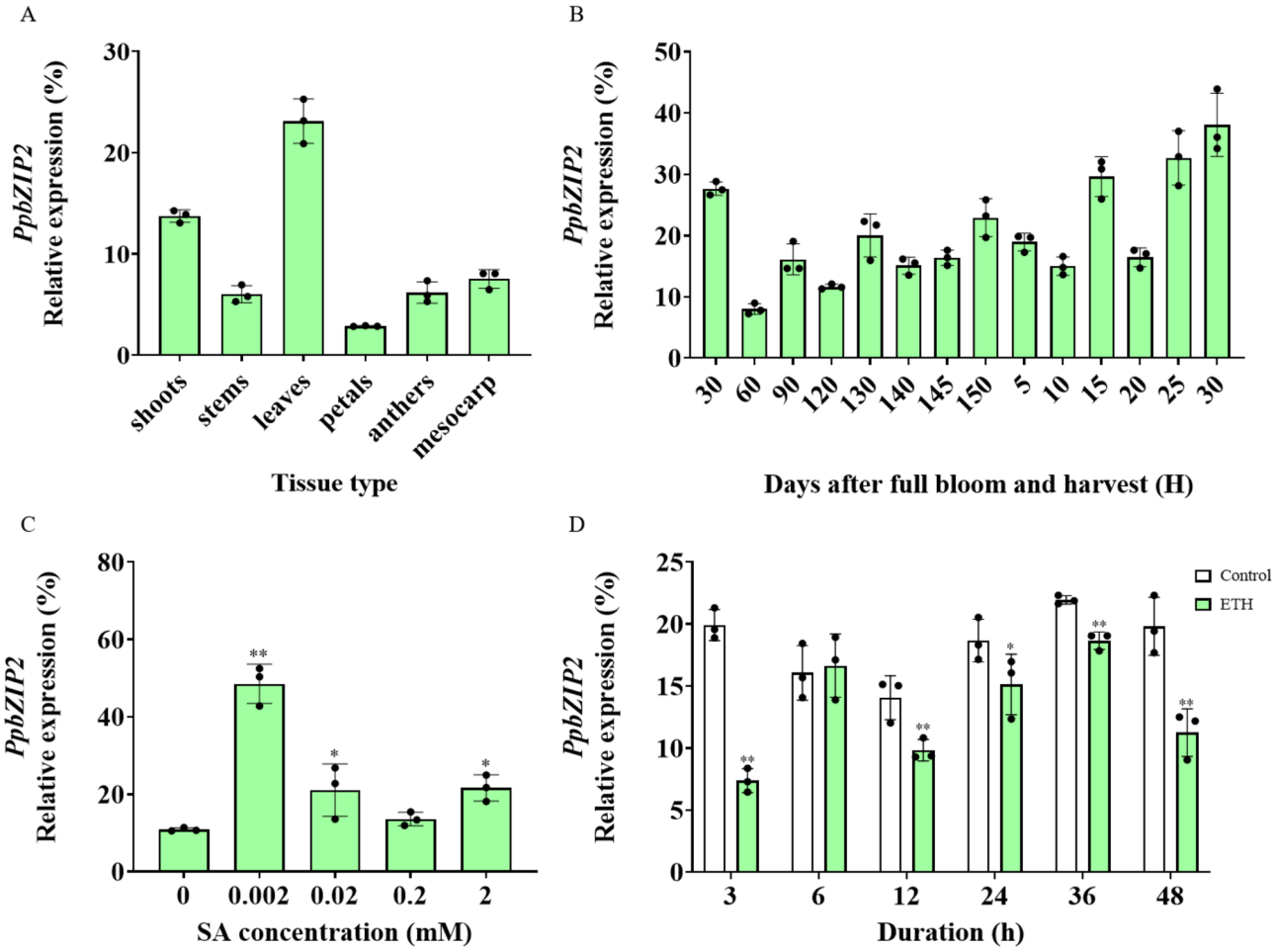

Fig. 9 Expression pattern of *PpBZIP2*. **A** The expression of *PpbZIP2* in various tissues of the 'Whangkeumbae'. **B** Changes in the expression of *PpbZIP2* during fruit development in 'Whangkeumbae'. **C** The regulatory effect of SA on the expression of *PpbZIP2*. **D** ETH on the expression of *PpbZIP2*

expression levels in the entire aerial part, indicating its potential broad functionality in various aerial organs. In contrast, the expression of these four genes in leaves is relatively low (Fig. 5), further emphasizing their tissue-specific expression bias. As observed in other plants, the expression patterns of the *MAPK* genes in sand pear exhibit significant tissue specificity. For example, in buckwheat, *FtMAPK1* and *FtMAPK3* are highly expressed in the roots, stems, and leaves. In watermelon, distinct expression patterns of *MAPK* genes are observed in the roots, stems, and leaves [45]. The dynamic and time-specific expression patterns of *PpMAPK* genes during the senescence of sand pear fruit were further characterized, uncovering their potential regulatory roles at distinct stages of this process. Notably, *PpMAPK3-L* and *PpMAPK10-L* exhibited peak expression at 25 DAH, suggesting their involvement in mid-stage senescence. *PpMAPK7-L* showed maximum expression at 30 DAH, indicating a role in the late phase of senescence. In contrast, *PpMAPK16-L* peaked as early as 5 DAH, implying that it may participate in early senescence-associated responses initiated at the onset of fruit development (Fig. 6). These findings highlight that different *PpMAPK* genes may contribute to multiple stages of pear fruit senescence through finely tuned temporal regulation, possibly via transcriptional modulation or signal transduction cascades, underscoring their diverse and complex functions within the senescence regulatory network.

This study further confirmed the crucial role of the MAPK signaling pathway in plant hormone responses, particularly its potential function in regulating fruit development and senescence. The results revealed that four representative *PpMAPK* genes exhibited distinct expression responses under various hormone treatments, with significant changes observed, especially in response to SA and ETH treatments (Fig. 7). These findings suggest that the PpMAPK pathway mediates the perception and transduction of hormone signals, playing a key role in regulating physiological processes such as fruit growth, maturation, and senescence. Additionally, the hormone response characteristics of *PpMAPK* genes highlight their central role in complex signaling

networks, potentially linking them to diverse biological processes, including stress resistance and tissue differentiation. The expression levels of four *PpMAPK* genes also showed significant differences between diseased fruit and control fruit. Specifically, the expression levels of PpMAPK3-L and PpMAPK10-L in fruit were significantly up-regulated, which may be related to disease-induced defense response. In contrast, the expression of PpMAPK7-L and PpMAPK16-L in diseased fruit was significantly lower than that in control, suggesting that they may play an important role in the maintenance of healthy fruit (Additional file 5: Fig. S3). These differences indicate that different *PpMAPK* genes may play a role in the mechanism of pear fruit disease resistance.

To further investigate the potential interaction mechanisms of MAPK genes in fruit senescence, this study first used the online tool STRING to predict possible interacting proteins of these MAPK genes (Additional file 2: Fig. S1). The predicted interactions were then validated using Y2H technology. The experimental results demonstrated an interaction between PpMAPK3-L and PpbZIP2 (Fig. 8). This finding is consistent with previous studies, which have shown that many MAPK members interact with transcription factors to play critical roles in various physiological processes in plants. In the complex biological process of fruit development, such interactions may serve as a key link between external signals and the regulation of gene expression. For instance, the interaction between MPK4 and MYB1 is crucial for regulating anthocyanin accumulation [46], while the interaction between MdERF17 and MdMPK4 is important at different stages of plant growth [47]. In sand pear fruit, the expression of *PpbZIP2* peaked at 30 DAH (Fig. 9B). Further experiments revealed that SA significantly induced *PpbZIP2* expression (Fig. 9C), while ETH treatment significantly suppressed it (Fig. 9D). These findings suggest that the expression of *PpbZIP2* is regulated by various signaling molecules. Additional mechanistic studies revealed that the interaction between PpbZIP2 and PpMAPK3-L may delay fruit senescence through synergistic effects, regulating the expression of senescence-related genes, thus providing new molecular mechanisms and research directions for preserving sand pear fruit.

In summary, this study revealed the potential function of the *MAPK* genes in fruit senescence and disease resistance regulation, and provided valuable clues for resolving the biological role of the *MAPK* genes in complex physiological processes of pear fruit. More importantly, these findings laid an important theoretical foundation for improving stress resistance, extending the shelf life, and improving the quality of fruit by molecular breeding in the future, and pointed out the direction for further research on the MAPK signaling pathway. Although the present study has confirmed that the MAPK pathway plays a critical role in pear fruit senescence, the entire signaling cascade has not been fully explored, nor have its potential interactions with other pathways been elucidated. To comprehensively uncover the regulatory mechanisms of MAPK signaling in fruit senescence, future studies should conduct more detailed investigations into the roles of MAPK signaling networks, including both upstream and downstream components.

Conclusion

This study provides an in-depth analysis of the PpMAPKs in 'Whangkeumbae' (*Pyrus pyrifolia*) through the integration of transcriptomic and genomic data. A total of 25 *PpMAPK* genes were identified, including four from transcriptomic data (*PpMAPK3-L*, *PpMAPK7-L*, *PpMAPK10-L*, and *PpMAPK16-L*) and 22 from genomic data. Further homologous sequence alignment revealed that the transcriptomic PpMAPKs (PpMAPK3-L, PpMAPK7-L, PpMAPK10-L, and PpMAPK16-L) shared high sequence identity with their corresponding genomic counterparts (EVM0007944.1, EVM0004426.1, EVM0027166.1, EVM0023771, EVM0028755.1, and EVM0015862.1), with identity values of 99.19%, 100%, 94.51%, and 95.75%, respectively. This indicates a high degree of consistency in gene identification between the transcriptomic and genomic data. These findings provide a solid data foundation for understanding the genetic characteristics of *MAPK* genes in *Pyrus pyrifolia*. Phylogenetic analysis revealed that the 25 PpMAPKs were classified into four subfamilies (A, B, C, and D). Subfamilies A and B each contained six members, subfamily C contained four members, and subfamily D comprised nine members. The potential functional differences among the gene members of each subfamily provide valuable insights for the study of MAPK signaling pathways. Further interaction analysis identified a significant interaction between PpMAPK3-L and the transcription factor PpbZIP2. Based on this finding, it is hypothesized that PpMAPK3-L and PpbZIP2 may jointly regulate fruit senescence in *Pyrus pyrifolia*, offering new perspectives for regulating the MAPK signaling pathway in plant senescence processes.

Materials and methods

Plant materials

In this study, *Pyrus pyrifolia* Nakai 'Whangkeumbae' cultivated at Hebei Agricultural University was selected as the experimental material. Fruit samples were tagged during the flowering stage to enable the tracking and evaluation of their physiological characteristics at different maturation stages. Fruits were harvested at 30, 60, 90, 120, 130, 140, 145 and 150 DAFB, representing sequential stages of fruit development. Immediately after harvesting, the fruit mesocarp was rapidly frozen in liquid

nitrogen to preserve physiological activity and prevent metabolic changes, then stored at − 80 °C in an ultra-low temperature freezer for subsequent analysis. In addition to fruits, samples of other tissues, including young shoots, stems, leaves, petals, and anthers were also collected and promptly stored at − 80 °C to maintain their physiological integrity prior to analysis.

To further investigate the effects of SA and ETH on fruit ripening under different conditions, mesocarp discs prepared from fruit collected at 150 DAFB were used for treatment. These discs were obtained using a cork borer and subsequently immersed in SA solutions at concentrations of 0.02, 0.2, and 2 mM for 12 h. Corresponding controls were immersed in distilled water under the same conditions. In a separate set of treatments, mesocarp discs from the same batch of fruit were exposed to ethylene gas at a concentration of 1 µL/L for 3, 6, 12, 24, 36, or 48 h. Controls for this group also consisted of mesocarp discs immersed in distilled water. All procedures, including mesocarp disc preparation, SA and ETH treatments, and RNA extraction, were performed in strict accordance with the experimental protocol and were independently repeated three times to ensure the reliability and reproducibility of the results.

Genome-wide identification of MAPK in sand Pear

In our previous investigation, four proteins containing the MAPK domain were discovered through transcriptome analysis of the 'Whangkeumbae' of *Pyrus pyrifolia*. For the current research, the genome assembly of the 'Cuiguan' cultivar of sand pear (*Pyrus pyrifolia*) (assembly ID: GWHBAOS00000000) was obtained from the NGDC database (https://ngdc.cncb.ac.cn/). Additionally, MAPK protein sequences from *Arabidopsis thaliana* were retrieved from the TAIR database (https://www.arabidopsis.org/). To identify MAPK gene family members in *Pyrus pyrifolia*, two complementary strategies were employed. Initially, the Hidden Markov Model (HMM) profile corresponding to the MAPK domain (PF03110) was downloaded from the Pfam database (http://pfam.xfam.org/) and aligned with the entire *Pyrus pyrifolia* proteome using TBtools-II to identify MAPK-related sequences [48]. In parallel, a comprehensive local BLASTP search was conducted using the MAPK protein sequences from *Arabidopsis thaliana* as queries, with an E-value cutoff of less than 10^{-5}, against the *Pyrus pyrifolia* genome to obtain putative PpMAPKs. Duplicated sequences identified in the results were excluded. Finally, the presence of conserved MAPK domains in the candidate PpMAPK proteins was confirmed by performing batch domain analysis via both the Pfam and NCBI-CDD databases (https://www.ncbi.nlm.nih.gov/Structure/cdd/wrpsb.cgi).

Phylogenetics analysis of PpMAPKs

A total of 22 MAPK family members were identified in sand pear, and 4 MAPK members were identified in transcriptome. The sequence similarity between PpMAPK7-L and EVM0004426.1 was 100%. To investigate the evolutionary relationships among MAPK family proteins, we utilized the NCBI BLASTP tool (https://www.ncbi.nlm.nih.gov/) to retrieve protein sequences from *Malus domestica*, *Solanum lycopersicum*, *Nicotiana tabacum*, and *Arabidopsis thaliana*. Multiple sequence alignment was carried out using the ClustalW algorithm to compare the MAPK protein sequences. Subsequently, a phylogenetic tree was generated using the Neighbor-Joining (NJ) method in MEGA version 7.0, with 1,000 bootstrap replicates to assess the reliability of the branches [49, 50]. The resulting phylogenetic tree was further refined and visualized using the online platform iTOL (https://itol.embl.de/).

Identification of physical and chemical properties of MAPK family members

TBtools was used to extract CDS sequences, protein sequences and promoter sequences of MAPK family members for subsequent analysis. On Expasy website (https://web.expasy.org/protparam/) protein hydrophobicity, molecular weight and pI were predicted. The online site Plant-mPLoc (http://www.csbio.sjtu.edu.cn/bioinf/plant-multi/) was used to predict the location of PpMAPKs [51]. To predict the putative interaction proteins of PpMAPKs, we utilized the STRING database (https://string-db.org/). As pear-specific data were unavailable, the analysis was performed based on homologs from *Malus domestica*, a closely related species.

Analysis of motifs, conserved domains and gene structure of PpMAPKs

The amino acid sequences of the PpMAPK proteins were analyzed using the NCBI Conserved Domain Database (NCBI-CDD) and the online MEME Suite (https://meme-suite.org/meme/index.html). These tools were employed to detect conserved domains and sequence motifs, using significance thresholds of E-value 0.01 for domain identification and E-value 0.05 for motif discovery. The genomic annotation file of *Pyrus pyrifolia* was obtained from NGDC and the gene structure was analyzed. The CDS sequences were compared with the corresponding genomic DNA sequences using the Gene Structure Display Server (GSDS) tool (http://gsds.cbi.pku.edu.cn/) to analyze the gene structure. The phylogenetic tree, conserved motifs, domains and gene structure diagrams of PpMAPK were constructed by using TBtools-II software.

Chromosome localization and promoter cis-acting elements of PpMAPK family

TBtools software was used to analyze the pear genome annotation file, determine the chromosome location information of each *PpMAPK* sequence, and draw the corresponding chromosome location map. Place the sequence obtained in TBtools at the first 2000 bp of the start codon ATG in the Plant CARE website (https://bioinformatics.psb.ugent.be/webtools/plantcare/html/). Hormone-related elements were screened among all cis-acting elements. The number of each cis-acting element was counted, the Heatmap tool of TBtools was used to classify and visually analyze promoters of PpMAPK family members. Map the Location of MAPK family members on chromosomes via using the Gene Location Visualize from GTF/GFF tool in TBtools. Artificial intelligence was used to beautify pictures.

RNA extraction and quantitative real-time polymerase chain reaction (qRT-PCR)

Total RNA was extracted from the pulp tissue using the DP210831RNAprep Pure Polysaccharide Polyphenol Plant Total RNA Extraction Kit (Tiangen Biotechnology Company Ltd, Beijing, China). For each sample, 0.1 g of tissue was used. RNA concentration was quantified with a NanoDrop 2000 microvolume spectrophotometer, and quality was assessed via the A260/A280 ratio. Subsequently, reverse transcription was accomplished to generate cDNA using the FastQuantcDNA First Strand Synthesis Kit (Tiangen Biotechnology Company Ltd, Beijing, China). Specifically, based on the measured RNA concentration, 50 ng to 2 μg of total RNA was combined on ice with 2 μL of 5× gDNA Buffer and RNase-Free ddH_2O to a final volume of 10 μL, mixed thoroughly, centrifuged briefly, and incubated at 42 °C for 3 min in a thermal cycler. The reverse transcription mix was prepared by combining 2 μL of 10× King RT Buffer, 1 μL of FastKing RT Enzyme Mix, 2 μL of FQ-RT Primer Mix, and RNase-Free ddH_2O to a final volume of 10 μL. This mix was then added to the pre-incubated RNA sample, followed by incubation at 42 °C for 15 min and subsequent inactivation at 95 °C for 3 min, yielding stable cDNA. Primers were designed using DNAMAN software, NCBI and Primer Premier software. The qPCR analysis was performed by a real-time polymerase chain reaction system. Each qPCR reaction was carried out in a total volume of 20 μL, comprising 10 μL of 2 × SYBR Mixture (Cwbio, Beijing, China), 0.4 μL of each primer (10 mmol/L), 7.2 μL of nuclease-free water, and 2 μL of diluted cDNA. The PCR procedure included an initial template predenaturation at 95 ℃ for 30 s, succeeded by 42 cycles of denaturation at 95 ℃ for 5 s, annealing at 60 ℃ for 30 s, and extension at 72 ℃ for 10 s. To ensure the specificity of the amplification, a melting curve analysis was performed. The relative quantification of gene expression was calculated using the POWER method. The fluorescence quantitative PCR instrument employed in this study was the Mastercycler ep realplex 4 (Eppendorf AG, Hamburg, Germany). The internal references utilised in this study were the *PpUBI* (GenBank number: AF195224) gene. Primers for RT-qPCR analysis are listed in Additional file 1 (Table S1).

Y2H assay

Complete coding DNA sequences (CDS) of *PpMAPK3-L*, *PpMAPK7-L*, *PpMAPK10-L*, and *PpMAPK16-L* were obtained based on BLAST analysis of the sand pear transcriptome database [30]. The recombinant plasmid *PpMAPK3-L*-pGBKT7, *PpMAPK7-L*-pGBKT7, *PpMAPK10-L*-pGBKT7, and *PpMAPK16-L*-pGBKT7 were successfully constructed by connecting PpMAPK3-L, PpMAPK7-L, PpMAPK10-L and PpMAPK16-L with the decoy vector pGBKT7, respectively. The CDS sequences of *PpbZIP2* and *PpbZIP3* were connected to the prey vector to construct *PpbZIP2*-pGADT7 and *PpbZIP3*-pGADT7. The constructed *PpMAPK3-L*-pGBKT7, *PpMAPK7-L*-pGBKT7, *PpMAPK10-L*-pGBKT7, and *PpMAPK16-L*-pGBKT7 plasmids were fused with *PpbZIP2*-pGADT7, PpbZIP3-pGADT7, respectively. The fusion plasmid was co-transferred to yeast AH109, and the transformed bacterial solution was coated on the yeast medium Trp and Leu. After incubation at 30℃ for 3 days, positive colonies were selected and strewed on SD/-Trp/-Leu and SD/-Trp/-Leu/-Ade/X-α-gal plates, respectively. Protein-protein interactions were observed after incubation at 30℃ for 3 days. Prey vectors and bait vectors without target sequences were used as negative control.

Data analysis

All experimental data are presented as the mean ± standard deviation (mean ± SD), with the data sourced from at least three biological replicates to ensure the representativeness and statistical robustness of the results. To assess significant differences between treatment groups in response variables, one-way analysis of variance (ANOVA) was used for statistical inference. For further analysis of significant differences, Duncan's multiple range test was employed to perform pairwise comparisons of mean differences between the treatment groups. Statistical significance was determined by the following criteria: $P < 0.05$ was considered statistically significant, and $P < 0.01$ was regarded as highly significant. All data were analyzed in SPSS v27.0 (IBM Corp., Armonk, NY, USA) (Table 1).

Abbreviations

MAPK	Mitogen-activated protein kinase
SA	Salicylic acid

Y2H	Yeast two-hybridization
TFs	Transcription factors
bZIP	Basic leucine zipper
Leu	Leucine
Ile	Isoleucine
Val	Valine
Phe	Phenylalanine
Met	Methionine
NCBI	National Center for Biotechnology Information
Da	Dalton
pI	Isoelectric points
DAH	Days after harvest
ETH	Ethephon
BD	pGBKT7
AD	pGADT7
SD/-Trp/-Leu	Synthetic dropout medium/-tryptophan/-leucine
SD/-Trp/-Leu/-His/-Ade/X-α-gal	SD/-Trp/-Leu/-histones/-adenine/X-alpha gal
DAFB	Days after full bloom
NGDC	National genome data center
HMM	Hidden Markov Model
NJ	Neighbor-joining
GSDS	Gene Structure Display Server
AI	Artificial Intelligence
CDS	Complete coding DNA sequences
qRT-PCR	Quantitative real-time polymerase chain reaction
SD	Standard deviation
ANOVA	Analysis of variance

Supplementary Information

The online version contains supplementary material available at https://doi.org/10.1186/s12864-025-11672-0.

Supplementary Material 1

Supplementary Material 2

Supplementary Material 3

Supplementary Material 4

Supplementary Material 5

Acknowledgements
The authors extend their gratitude to Professor Chen Liang (Chinese Academy of Sciences) for his valuable assistance with providing the yeast two-hybrid vectors.

Author contributions
SHY formulated the research topic. SHY, XY, and WHY analyzed data and interpreted the results. SHY and XY wrote the manuscript. SHY, XY and WHY revised the manuscript. All authors read and approved the final manuscript.

Funding
This work was supported by the National Natural Science Foundation of China (32272654), Hebei Natural Science Foundation, China (C2023204016), the Hebei Province Introduced Overseas-Scholar Fund, China (C20220361), and the Hebei Province Outstanding Youth Fund, China (2016, 2019).

Data availability
Data is provided within the manuscript.

Declarations

Ethics approval and consent to participate
The 'Whangkeumbae' was used in the current study was obtained from the experimental farm of Hebei Agricultural University, China. All the required permissions have been obtained, and all the plant materials during the current study were provided free of charge and maintained following the international guidelines.

Consent for publication
Not applicable.

Competing interests
The authors declare no competing interests.

Author details
[1]College of Horticulture, Hebei Agricultural University, Baoding, Hebei 071001, China

Received: 3 March 2025 / Accepted: 5 May 2025
Published online: 15 May 2025

References

1. Liang CZ, Zheng GY, Li WZ, Wang YQ, Hu B, Wang HR, et al. MT delays leaf senescence and enhances salt stress tolerance in rice. J Pineal Res. 2015;59(1):91–101.
2. Gapper NE, Mcquinn RP, Giovannoni JJ. Molecular and genetic regulation of fruit ripening. Plant Mol Biol. 2013;82(6):575–91.
3. Adams-Phillips L, Barry C, Giovannoni J. Signal transduction systems regulating fruit ripening. Trends Plant Sci. 2004;9(7):331–8.
4. Raskin I. Salicylate, a new plant hormone. Plant Physiol. 1992;99(3):799–803.
5. Clarke SM, Mur LAJ, Wood JE, Scott IM. Salicylic acid dependent signaling promotes basal thermotolerance but is not essential for acquired thermotolerance in *Arabidopsis thaliana*. Planta. 2004;38(3):432–47.
6. Asghari M, Aghdam MS. Impact of Salicylic acid on post-harvest physiology of horticultural crops. Trends Food Sci Technol. 2010;21(10):502–9.
7. Jiang M, Zhang YZ, Li P, Jian JJ, Zhao CL, Wen GS. Mitogen-activated protein kinase and substrate identification in plant growth and development. Int J Mol Sci. 2022;23(5):2744.
8. Group M. Mitogen-activated protein kinase cascades in plants: a new nomenclature. Trends Plant Sci. 2002;7(7):301–8.
9. Liu YK, Zhang D, Wang L, Li DQ. Genome-wide analysis of mitogen activated protein kinase gene family in maize. Plant Mol Biol Rep. 2013;31(6):1446–60.
10. Majeed Y, Zhu X, Zhang N, Ul-Ain N, Raza A, Haider FU, et al. Harnessing the role of mitogen-activated protein kinases against abiotic stresses in plants. Front Plant Sci. 2023;14:932923.
11. Asif MH, Lakhwani D, Pathak S, Bhambhani S, Bag SK, Trivedi PK. Genome wide identification and expression analysis of the mitogen-activated protein kinase gene family from banana suggest involvement of specific members in different stages of fruit ripening. Funct Integr Genomics. 2014;14(1):161–75.
12. Zhang SZ, Xu RR, Luo XC, Jiang ZS, Shu HR. Genome-wide identification and expression analysis of MAPK and MAPKK gene family in *Malus domestica*. Gene. 2013;531(2):377–87.
13. Kong FL, Wang J, Cheng L, Liu SY, Wu J, Peng Z, et al. Genome-wide analysis of the mitogen-activated protein kinase gene family in *Solanum lycopersicum*. Gene. 2012;499(1):108–20.
14. Wang J, Pan CT, Wang Y, Ye L, Wu J, Chen LF, et al. Genome-wide identification of MAPK, MAPKK, and MAPKKK gene families and transcriptional profiling analysis during development and stress response in cucumber. BMC Genomics. 2015;16(1):386.
15. Jonak C, Okrész L, Bögre L, Hirt H. Complexity, cross talk and integration of plant MAP kinase signalling. Curr Opin Plant Biol. 2002;5(5):415–24.
16. Wu CJ, Shan W, Liu XC, Zhu LS, Wei W, Yang YY, et al. Phosphorylation of transcription factor bZIP21 by MAP kinase MPK6-3 enhances banana fruit ripening. Plant Physiol. 2022;188(3):1665–85.
17. Wang FX. The molecular mechanisms of the MAPK5-OsWRKY72 module for regulating grain length and salt stress in rice. Fujian Agriculture and Forestry University; 2024.
18. Huang X, Wei JM, Feng WZ, Luo Q, Tan GF, Li YZ. Interaction between SlMAPK3 and SlASR4 regulates drought resistance in tomato (*Solanum lycopersicum* L). Mol Breed. 2023;43(10):73.
19. Liu YD, Zhang SQ. Phosphorylation of 1-aminocyclopropane-1-carboxylic acid synthase by MPK6, a stress-responsive mitogen-activated protein kinase, induces ethylene biosynthesis in *Arabidopsis*. Plant Cell. 2004;16(12):3386–99.

20. Lehti-Shiu MD, Panchy N, Wang P, Uygun S, Shiu SH. Diversity, expansion, and evolutionary novelty of plant DNA-binding transcription factor families. Biochim Biophys Acta Gene Regul Mech. 2017;1860(1):3–20.
21. Nijhawan A, Jain M, Tyagi AK, Khurana JP. Genomic survey and gene expression analysis of the basic leucine zipper transcription factor family in rice. Plant Physiol. 2008;146(2):333–50.
22. Wang XG, Lu XK, Malik WA, Chen XG, Wang JJ, Wang DL, et al. Differentially expressed bZIP transcription factors confer multi-tolerances in *Gossypium hirsutum* L. Int J Biol Macromol. 2020;146:569–78.
23. Sornaraj P, Luang S, Lopato S, Hrmova M. Basic leucine zipper (bZIP) transcription factors involved in abiotic stresses: a molecular model of a wheat bZIP factor and implications of its structure in function. Biochim Biophys Acta. 2016;1860(1):46–56.
24. Dröge-Laser W, Weiste C. The C/S 1 bZIP network: a regulatory hub orchestrating plant energy homeostasis. Trends Plant Sci. 2018;23(5):422–33.
25. Lovisetto A, Guzzo F, Tadiello A, Confortin E, Pavanello A, Botton A, et al. Characterization of a *bZIP* gene highly expressed during ripening of the Peach fruit. Plant Physiol Biochem. 2013;70:462–70.
26. Hou HY, Kong XJ, Zhou YJ, Yin CX, Jiang YM, Qu HX, et al. Genome-wide identification and characterization of bZIP transcription factors in relation to litchi (*Litchi chinensis* Sonn.) fruit ripening and postharvest storage. Int J Biol Macromol. 2022;222:2176–89.
27. Weiste C, Pedrotti L, Selvanayagam J, Muralidhara P, Fröschel C, Novák O, et al. The *Arabidopsis* bZIP11 transcription factor links low-energy signalling to auxin-mediated control of primary root growth. PLoS Genet. 2017;13(2):e1006607.
28. Ma HZ, Liu C, Li ZX, Ran QJ, Xie GN, Wang BM, et al. ZmbZIP4 contributes to stress resistance in maize by regulating ABA synthesis and root development. Plant Physiol. 2018;178(2):753–70.
29. Bastías A, Yañez M, Osorio S, Arbona V, Gómez-Cadenas A, Fernie AR, et al. The transcription factor AREB1 regulates primary metabolic pathways in tomato fruits. J Exp Bot. 2014;65(9):2351–63.
30. Shi HY, Cao LW, Xu Y, Yang X, Liu SL, Liang ZS et al. 2021. Transcriptional profiles underlying the effects of salicylic acid on fruit ripening and senescence in pear (*Pyrus pyrifolia* Nakai). J Integr Agric. 2021;20(9):2424–37.
31. Gao YH, Yang QS, Yan XH, Wu XY, Yang F, Li JZ, et al. High-quality genome assembly of 'cui Guan' Pear (*Pyrus pyrifolia*) as a reference genome for identifying regulatory genes and epigenetic modifications responsible for bud dormancy. Hortic Res. 2021;8(1):197.
32. Kim HS, Park SC, Ji CY, Park S, Jeong JC, Lee HS, Kwak SS. Molecular characterization of biotic and abiotic stress-responsive MAP kinase genes, *IbMPK3* and *IbMPK6*, in sweetpotato. Plant Physiol Biochem. 2016;108:37–48.
33. Chen J, Wang LH, Yuan M. Update on the roles of rice MAPK cascades. Int J Mol Sci. 2021;22(4):1679.
34. Singh A, Nath O, Singh S, Kumar S, Singh IK. Genome-wide identification of the *MAPK* gene family in Chickpea and expression analysis during development and stress response. Plant Gene. 2017;13:25–35.
35. Wang G, Wang T, Jia ZH, Xuan JP, Pan DL, Guo ZR, et al. Genome-wide bioinformatics analysis of MAPK gene family in Kiwifruit (*Actinidia Chinensis*). Int J Mol Sci. 2018;19(9):2510.
36. Cui LC, Yang G, Yan JL, Pan Y, Nie XJ. Genome-wide identification, expression profiles and regulatory network of MAPK cascade gene family in barley. BMC Genomics. 2019;20(1):750.
37. Zhang XY, Wang LM, Xu XY, Cai CP, Guo WZ. Genome-wide identification of mitogen-activated protein kinase gene family in *Gossypium raimondii* and the function of their corresponding orthologs in tetraploid cultivated cotton. BMC Plant Biol. 2014;14:345.
38. Zhan HS, Hong Y, Zhao X, Wang M, Song WN, Nie XJ. Genome-wide identification and analysis of MAPK and MAPKK gene families in bread wheat (*Triticum aestivum* L). Genes. 2017;8(10):284.
39. Zhou HY, Ren SY, Han YF, Zhang Q, Qin L, Xing Y. Identification and analysis of mitogen-activated protein kinase (MAPK) cascades in *Fragaria vesca*. Int J Mol Sci. 2017;18(8):1766.
40. Yao YJ, Zhao HX, Sun L, Wu WJ, Li CL, Wu Q. Genome-wide identification of MAPK gene family members in *Fagopyrum tataricum* and their expression during development and stress responses. BMC Genomics. 2022;23(1):96.
41. Chen LH, Hu W, Tan SD, Wang M, Ma ZB, Zhou SY, et al. Genome-wide identification and analysis of MAPK and MAPKK gene families in *Brachypodium distachyon*. PLoS ONE. 2012;7(10):e46744.
42. Zhang XT, Cheng TC, Wang GH, Yan YF, Xia QY. Cloning and evolutionary analysis of tobacco MAPK gene family. Mol Biol Rep. 2012;40(2):1407–15.
43. Nicole MC, Hamel LP, Morency MJ, Beaudoin N, Ellis BE, Séguin A. MAP-ping genomic organization and organ-specific expression profiles of Poplar MAP kinases and MAP kinase kinases. BMC Genomics. 2006;71:223.
44. Neupane A, Nepal MP, Piya S, Subramanian S, Rohila JS, Reese RN, et al. Identification, nomenclature, and evolutionary relationships of mitogen-activated protein kinase (MAPK) genes in soybean. Evol Bioinform Online. 2013;9:363–86.
45. Song QM, Li DY, Dai Y, Liu SX, Huang L, Hong YB, et al. Characterization, expression patterms and functional analysis of the *MAPK* and *MAPKK* genes in watermelon (*Citrullus lanatus*). BMC Plant Biol. 2015;15(1):298–315.
46. Yang T, Ma HY, Li Y, Zhang Y, Zhang J, Wu T, et al. Apple MPK4 mediates phosphorylation of MYB1 to enhance light-induced anthocyanin accumulation. Plant J. 2021;106(6):1728–45.
47. Wang S, Wang T, Li QQ, Xu C, Tian J, Wang Y, et al. Phosphorylation of MdERF17 by MdMPK4 promotes Apple fruit Peel degreening during light/dark transitions. Plant Cell. 2022;34(5):1980–2000.
48. Chen CJ, Chen H, Zhang Y, Thomas HR, Frank MH, He Y, et al. TBtools: an integrative toolkit developed for interactive analyses of big biological data. Mol Plant. 2020;13(8):1194–202.
49. Kumar S, Stecher G, Tamura K. MEGA7: molecular evolutionary genetics analysis version 7.0 for bigger datasets. Mol Biol Evol. 2016;33(7):1870–4.
50. Saitou N, Nei M. The neighbor-joining method: A new method for reconstructing phylogenetic trees. Mol Biol Evol. 1987;4(4):406–25.
51. Chou KC, Shen HB. Plant-mPLoc: a top-down strategy to augment the power for predicting plant protein subcellular localization. PLoS ONE. 2010;5(6):e11335.

Publisher's note